Functional Connectome Organization Predicts Conversion to Psychosis in Clinical High-Risk Youth from the SHARP Program

Guusje Collin, MD, PhD [1,2,3]; Larry J. Seidman, PhD [1,†]; Matcheri S. Keshavan, MD [1]; William S. Stone, PhD [1]; Zhenghan Qi, MD, PhD [1,4]; Tianhong Zhang, MD, PhD [5]; Yingying Tang, PhD [5]; Huijun Li, PhD [6]; Sheeba Arnold Anteraper, PhD [2,7]; Margaret A. Niznikiewicz, PhD [8]; Robert W. McCarley, MD [8,†]; Martha E. Shenton, PhD [3,9,10]; Jijun Wang, MD [5]; Susan Whitfield-Gabrieli, PhD [2,11]

[1] Department of Psychiatry, Beth Israel Deaconess Medical Center, Harvard Medical School, Boston, MA, USA; [2] McGovern Institute for Brain Research, Department of Brain and Cognitive Sciences, Massachusetts Institute of Technology, Cambridge, MA, USA; [3] Psychiatry Neuroimaging Laboratory, Department of Psychiatry, Brigham and Women's Hospital, Harvard Medical School, Boston, MA, USA; [4] Department of Linguistics and Cognitive Science, University of Delaware, Newark, DE, USA; [5] Shanghai Key Laboratory of Psychotic Disorders, Shanghai Mental Health Center, Shanghai Jiao Tong University School of Medicine, Shanghai, China; [6] Florida A&M University, Department of Psychology, Tallahassee, FL, USA; [7] Alan and Lorraine Bressler Clinical and Research Program for Autism Spectrum Disorder, Massachusetts General Hospital, Boston MA, USA; [8] Department of Psychiatry, VA Boston Healthcare System, Brockton Division, Brockton, MA, USA; [9] Research and Development, VA Boston Healthcare System, Brockton Division, Brockton, MA, USA; [10] Department of Radiology, Brigham and Women's Hospital, Harvard Medical School, Boston, MA, USA; [11] Poitras Center for Affective Disorders, Department of Brain and Cognitive Sciences, Massachusetts Institute of Technology, Cambridge, MA, USA

Collin, G., Seidman, L.J., Keshavan, M.S., Stone, W.S., Qi, Z., Zhang, T., Tang, Y., Li, H., Anteraper, S.A., Niznikiewicz, M.A., McCarley, R.W., Shenton, M.E., Wang, J., Whitfield-Gabrieli, S., 2018. Functional connectome organization predicts conversion to psychosis in clinical high-risk youth from the SHARP program. Mol. Psychiatry. https://doi.org/10.1038/s41380-018-0288-x

Corresponding author

Guusje Collin, Beth Israel Deaconess Medical Center, Department of Psychiatry, Massachusetts Mental Health Center, 75 Fenwood Road, Boston, MA 02115, USA; Phone: +1 (617) 626 9300; Email: gcollin@bidmc.harvard.edu.

JiJun Wang, Shanghai Key Laboratory of Psychotic Disorders, Shanghai Mental Health Center, Shanghai Jiao Tong University School of Medicine, 600 Wanping Nan Road, Shanghai, 200030, China. Phone: +86 (21) 3477 3065. Email: jijunwang27@163.com.

Running title

Connectome Organization Predicts Conversion to Psychosis

Abstract

The emergence of prodromal symptoms of schizophrenia and their evolution into overt psychosis may stem from an aberrant functional reorganization of the brain during adolescence. To examine whether abnormalities in connectome organization precede psychosis onset, we performed a functional connectome analysis in a large cohort of medication-naïve youth at risk for psychosis from the Shanghai At Risk for Psychosis (SHARP) study. The SHARP program is a longitudinal study of adolescents and young adults at Clinical High Risk (CHR) for psychosis, conducted at the Shanghai Mental Health Center in collaboration with neuroimaging laboratories at Harvard and MIT. Our study involved a total of 251 subjects, including 158 CHRs and 93 age-, sex-, and education-matched healthy controls. During one-year follow-up, 23 CHRs developed psychosis. CHRs who would go on to develop psychosis were found to show abnormal modular connectome organization at baseline, while CHR non-converters did not. In all CHRs, abnormal modular connectome organization at baseline was associated with a three-fold conversion rate. A region-specific analysis showed that brain regions implicated in early-course schizophrenia, including superior temporal gyrus and anterior cingulate cortex, were most abnormal in terms of modular assignment. Our results show that functional changes in brain network organization precede the onset of psychosis and may drive psychosis development in at-risk youth.

Introduction

Schizophrenia is a psychiatric disorder that manifests early in life and derails social, cognitive, and academic development. The development of the illness typically follows a sequential trajectory that includes a premorbid phase with subtle and nonspecific deviations from normative development, [1] a prodromal phase with sub-threshold symptoms and declining functioning, [2–4] and a first psychotic episode that marks the formal onset of the illness. [5] In recent years, the focus of schizophrenia research shifted from the first episode to earlier stages of illness development. Studies of the prodromal phase aim to elucidate the biological and environmental factors that guide the trajectory from elevated risk to established illness, in order to contribute to the development of early detection and intervention strategies for schizophrenia. [6]

The prodromal or clinical high risk (CHR) phase of schizophrenia is characterized by attenuated or transient psychotic symptoms such as unusual thought content, suspiciousness, or mild perceptual abnormalities that typically manifest in adolescence or early adulthood. [2,4] The CHR syndrome has a large heterogeneity in clinical outcome ranging from complete remission to full-blown psychosis. [7,8] It has been suggested that inter-individual differences in brain circuitry may underlie the differences in outcome for high-risk individuals. [9] Indeed, recent studies suggest that abnormalities in functional brain connectivity and organization may differentiate at-risk individuals who will develop psychosis from those who do not transition. [9,10] These studies may help to elucidate the neurobiological events that precipitate and possibly drive the manifestation of psychotic symptoms.

The typical timing of the CHR syndrome in middle to late adolescence coincides with a crucial phase of brain development during which psychosocial factors interact with genetically

mediated brain changes to reshape the brain's functional organization. The brain is organized into a collection of functional networks that form identifiable modules in the brain's network. [11] This modular organization is thought to allow specialized circuits to focus on specific tasks by limiting the interference of regions processing different types of neural information. [12,13] Neuroimaging studies indicate that a considerable reorganization of the brain's functional modules takes place between late childhood and early adulthood. [11,14,15] We hypothesize that the modular reorganization of the brain during this developmental window may go awry in at-risk youth, resulting in aberrant connectivity patterns that may contribute to the development of psychotic symptoms. [16]

To examine modular brain organization in at-risk youth, we draw from the field of connectomics, an emerging branch of neuroscience that uses graph theory to examine the brain's connectivity network known as the connectome. [17] By assessing the modular organization of the functional connectome in a large sample of adolescents and young adults at risk for psychosis, we aim to determine whether abnormalities in modular connectome organization exist before the onset of psychosis and predispose to psychotic convergence.

Materials and methods

Participants

This study involved a total of 251 participants, including 158 Clinical High Risk (CHR) subjects and 93 Healthy Controls (HC) matched to CHRs based on age, sex, and education in years. The large majority of CHRs was naïve to psychotropic medication at baseline clinical assessment (>95%) and neuroimaging (>80%). Participants were recruited at the Shanghai Mental Health Center (SMHC), as part of the Shanghai At Risk for Psychosis (SHARP) program. [18] This

NIMH-funded study is a collaboration between SMHC, Harvard Medical School at Beth Israel Deaconess Medical Center (BIDMC) and Brigham and Women's Hospital, and Massachusetts Institute of Technology (study details including power analysis and in/exclusion criteria in Supplementary Information 1.1). The study was approved by Institutional Review Boards of BIDMC and SMHC. All subjects or their legal guardians gave written informed consent. Table 1 provides demographic and clinical characteristics of all participants.

Clinical and cognitive assessment

Prodromal symptoms were assessed using a validated Chinese version [19] of the Structured Interview for Prodromal Symptoms (SIPS). [20] Total IQ was estimated using the Wechsler Abbreviated Scale of Intelligence (WASI). [21]

Conversion criteria

During a mean (sd) follow-up of 392 (77) days, 23 CHRs developed psychosis (CHR+), while 135 did not (CHR-). Conversion to psychosis was determined using the SIPS operational definition of psychosis onset, [22] with at least one psychotic level symptom (rated "6" on the SIPS positive scale) with either sufficient frequency or duration. For CHR+, the date of conversion was recorded and time to psychosis computed as the number of days between study inclusion and psychosis onset.

Image acquisition

Magnetic Resonance Imaging (MRI) scans were acquired on a 3T Siemens MR B17 (Verio) system, 32-channel head coil at the SMHC and included an anatomical T1-weighted MRI scan (MP-RAGE; TR=2300 ms, TE=2.96 ms, FA=9 degree, FOV=256mm, voxel size: 1x1x1mm, 192 contiguous sagittal slices, duration 9'14'') and resting-state fMRI (rs-fMRI) scan (149 functional volumes; TR=2500 ms, TE=30 ms, FA=90 degree, FOV=224mm, measurements=149, voxel size: 3.5x3.5x3.5mm, 37 contiguous axial slices, duration 6'19'').

Image preprocessing

Figure 1 provides an overview of all analysis steps. As connectivity and connectome metrics are sensitive to methodological factors including image preprocessing and node selection, [23,24] two processing streams were used to process our data to ensure that results were not specific to any one methodology (Figure 1A): a *surface-based* method, the results of which are presented as primary findings, and an *MNI-based* method used to verify primary findings.

Image processing is described in detail in Supplementary Information 1.2. Briefly, FreeSurfer (v6.0) [25] and CONN (v17d) [26] software were used to preprocess T1 and rs-fMRI data. For *surface-based* processing, a total of 162 subject-specific ROIs derived from FreeSurfer were used as nodes, including 148 regions comprising the Destrieux Atlas and 14 subcortical structures (bilateral thalamus, hippocampus, amygdala, nucleus accumbens, caudate nucleus, putamen and global pallidus). For *MNI-based* processing, T1 and rs-fMRI scans were normalized to MNI space and the Harvard-Oxford Atlas was used to divide the cerebrum into a total of 105 brain regions, [27] including 91 cortical brain regions and the same 14 subcortical structures. Rigorous

motion correction and artifact removal were performed to deal with spurious correlations. [26] There were no significant group-differences in motion parameters or the number of rejected fMRI volumes (Supplementary Information 1.2).

Functional connectome reconstruction

A functional connectome was constructed for each participant, consisting of 162 subject-specific (or 105 atlas-based) nodes representing the aforementioned brain regions. The level of functional connectivity between each node pair was computed as the normalized z-score of the Pearson's correlation between the noise-corrected timeseries of each pair of brain regions and stored in a functional connectivity matrix (Figure 1B).

Modular organization of the functional connectome

Various methods exist to examine the modular organization of complex networks. [13] Here, we use the Louvain community detection method (https://sites.google.com/site/bctnet/), which partitions a network so as to maximize metric Q, representing the strength of edges inside communities relative to edges between communities. [28] The method is suitable for functional connectome analysis as it can take both positive and negative edge weights (i.e., connectivity estimates) into account without requiring an arbitrary connectivity threshold. [13,28,29]

Group-networks. As a first step to assess the modular organization of the functional connectome, one group-averaged functional network was constructed for HC, CHR-, and CHR+ groups. Each group-network's modular organization was assessed using the Louvain method. As the algorithm searches for high modularity partitions in a heuristic fashion, resulting partitions

differ slightly from run to run. [13,29,30] Therefore, the algorithm was run 10,000 times for each group-network and the partition associated with the highest level of Q selected (Figure 1C). A consensus similarity method [31] was used as an alternative method to select modular partitions for both group and individual networks (Supplementary Information 1.3).

Individual subjects. Second, the Louvain algorithm was applied to individual connectome reconstructions. To assess how similar the modular organization of each individual network was to an average healthy network, network partitions of individual subjects were compared to the group-averaged HC network using the Rand similarity coefficient (S_R), [32] providing an intuitive measure (between 0 and 1) of the similarity between two partitions (details in Supplementary Information 1.3). Network resolution parameter γ was set to 1.5, in order to identify more fine-grained modules while not overinflating the total number of modules, as this would hamper comparisons of network partitions. [32] In addition, modular organization was examined across a range of γ (Supplementary Information 1.3).

Region-specific alterations in modular connectome organization

As an exploratory analysis to assess which brain regions are most abnormal in terms of module assignment in CHR+ versus CHR-, individual networks were again compared to the HC network, now determining for each node i in the network the fraction of neighboring nodes with equal module assignment (details in Supplementary Information 1.3).

Code availability

All image processing and graph analyses were performed using freely available software. Version and access details are provided in Supplementary Information 1.2 and 1.3.

Statistical analysis

Group analysis. Analysis of Covariance (ANCOVA) was used to compare S_R among subject groups. Assumptions of normality and homogeneity of variance were met (Supplementary Information 1.4). Age, sex, and the number of rejected fMRI volumes were included in the model as covariates, and group-covariate interactions were assessed. Medication status was included as a covariate of non-interest as a minority of CHRs (<20%) were on psychotropic medication by the time of scanning. Region-specific metrics were analyzed using the same ANCOVA model, applying FDR-correction (q = .05) to account for multiple comparisons.

Psychosis-free survival analysis. To determine whether abnormal modular connectome organization at baseline predicted conversion to psychosis, CHRs were divided by median split into two groups with above and below-average S_R, reflecting normal and abnormal modular organization respectively. Kaplan Meier analysis was used to assess psychosis-free survival for each group. Survival functions were compared using log-rank tests. Cox regression analysis was used to assess how baseline modular organization and clinical characteristics (i.e., age, sex, IQ, SIPS symptoms, and GAF functioning) predicted time to conversion.

Results

Modular connectome organization – group-networks

Figure 2a shows the modular organization of group-averaged functional networks. Community detection in the HC network yielded five modules, largely reflecting known functional networks. Modular organization of the CHR- network was similar to HCs. The CHR+ network showed a number of qualitative differences, including a separation of orbitofrontal regions from the (para)limbic module, and with bilateral superior temporal gyrus changing assignment from the sensorimotor to the (para)limbic module. Moreover, a sixth cingulo-opercular module was observed in the CHR+ network. This module was not present in HC and CHR+ group-networks at this resolution but did show up at higher levels of network resolution (Supplementary Figure 2). Using consensus similarity to identify modular partitions produced highly similar partitions (Supplementary Information 1.3).

Modular connectome organization – individual subjects

The Rand similarity coefficient, reflecting how similar the modular organization of individual networks was to the averaged healthy network, showed a significant main effect of group ($F_{(2, 245)} = 4.08$, $p = .018$). Post-hoc bivariate comparison indicated that modular partitions of CHR+ subjects were significantly less similar to the average healthy network than both HCs ($F_{(1, 110)} = 4.32$, $p = .039$) and CHR- ($F_{(1, 152)} = 7.87$, $p = .006$) (Figure 2b). There was no significant difference between HCs and CHR- $F_{(1, 222)} = 0.02$, $p = .898$). An additional analysis to ensure that HC results were not biased by the fact that individual HCs contributed to the group-averaged HC network confirmed our findings (Supplementary Information 1.3). Repeating the analyses using

the MNI-based processing method largely corroborated our findings (details in Supplementary Information 1.3 and Supplementary Figure 3 and 4). Consensus partitions were very similar to the original partitions and reanalysis of our main finding using consensus partitions produced a trend-level effect but did not change the nature of our findings (Supplementary Information 1.3). Assessing group-effects across different levels of resolution parameter γ showed that the main effect holds for a range of γ (see Supplementary Information 1.3 and Supplementary Figure 1 and 2). Of note, there were no significant group-differences in the overall level of modularity Q ($F_{(2,250)} = 1.08$, $p = .340$) or overall connectivity strength ($F_{(2,250)} = 1.7$, $p = .185$).

Region-specific alterations in modular organization

Using *surface-based* data, no regional effects survived FDR-correction. Using *MNI-based* data, the right superior temporal gyrus (STG) was the only region surviving FDR-correction ($F_{(1, 152)} = 9.20$, $p < .001$). As exploratory results, regional effects at uncorrected $p < .05$ from the *surface-based* and *MNI-based* analysis are summarized in Figure 3a and 3b respectively. Regions with (marginal) effects in both atlases included bilateral STG and temporal plane, and right anterior cingulate gyrus, fusiform cortex, and amygdala.

Psychosis-free survival analysis

Kaplan-Meier analysis indicated significantly different ($z = 2.41$, $p = .016$) psychosis-free survival functions for CHRs with typical versus atypical modular connectome organization (Figure 4), with a hazard ratio of 3.1 indicating a three-fold relative event rate (i.e. conversion to psychosis) in CHRs with atypical modular organization at baseline. Combining baseline S_R with

baseline clinical characteristics in one cox regression model indicated that abnormal baseline connectome organization (z = -2.37, p = .018), lower IQ (z = -2.48, p = .013) and male sex (z = 1.92, p = .036) predicted shorter time to conversion. These findings were confirmed using MNI-processed data (Supplementary Information 1.5 and Supplementary Figure 4).

Discussion

This study examined functional connectome organization in a large cohort of adolescents and young adults at clinical high-risk for psychosis. Our findings suggest that abnormalities in the modular organization of the functional connectome precede the first psychotic episode. We find that baseline modular connectome organization is abnormal in CHRs who go on to develop psychosis, but not in CHRs who do not convert. Moreover, conversion to psychosis was over three times more likely in CHRs with abnormal connectome organization at baseline as compared to CHRs with typical baseline connectome organization. Functional changes in brain network organization that precede the formal onset of psychosis may be involved in the manifestation of (prodromal) psychotic symptoms.

Our findings of abnormal modular organization of the functional connectome in youth at risk for schizophrenia are supported by three previous graph analytical studies of functional connectivity data in schizophrenia patients and at-risk youth. Two studies in schizophrenia patients demonstrated a reorganization of modular brain network topology in patients with established illness. [33,34] In addition, a recent study in 88 at-risk individuals, including 12 who later developed psychosis, identified changes in the modular organization of the functional connectome in at-risk subjects who transitioned to psychosis. [9] Our current study confirms and

extends these previous results by showing that abnormal functional organization of the connectome precedes the first psychotic episode and develops in the absence of psychotropic medication.

Two competing hypotheses have been developed on modular brain network organization in schizophrenia. The first is that the connectome is *more* modular in schizophrenia. An early version of this theory was proposed by Hoffman and McGlashan, who modeled the effects of excessive pruning in neural network simulations. They concluded that the resulting fragmentation of the brain network gives rise to functionally autonomous modules that act as 'parasitic foci' that repeatedly introduce the same output into the brain's information flow, which may underlie auditory hallucinations or delusions of control. [35–37] The second hypothesis, first articulated in a critique of Hoffman and McGlashan's work, argues that the brain's network is *less* modular in schizophrenia. [38] A less modular network could result in reduced information encapsulation and "overflow" of neural information from e.g., language into perceptual systems, and thereby invoke symptoms such as thought insertion and auditory hallucinations. Empirical evidence appears to favor the first theory, with a functional connectivity study showing more and smaller modules in schizophrenia patients [39] and two structural connectome studies showing higher modularity in schizophrenia and CHR. [40,41] In contrast, a study showing reduced modularity of functional brain networks in childhood-onset schizophrenia is more in line with the second theory. [42] Our current findings and previous results [33,34] add a third possibility. Namely, that the brain is not just more or less modular, but that there is a qualitative reorganization of the brain's modular organization in schizophrenia, resulting in abnormal functional interaction patterns between a range of brain regions, which may contribute to psychotic and cognitive symptom development.

Finding abnormalities in modular connectome organization before the onset of psychosis suggests that a maladaptive reorganization in the modular topology of the functional connectome may take place in the months to years preceding the first psychotic episode. In typical brain development, the maturation of different functional systems occurs at different times in the course of development, with e.g., sensorimotor networks maturing before those mediating higher cognitive functions. [43] Adolescent behaviors such as impulsivity and risk taking have been attributed to the asynchronous maturation of limbic and prefrontal systems, giving rise to heightened sensitivity to motivational cues in the context of immature cognitive control. [44] This critical window of limbic and cognitive system development and high sensitivity to socio-environmental inputs may represent a window of vulnerability for youth at risk for psychosis. Any deviation from the process of modular reorganization during this developmental window could give rise to complex patterns of hypo- and hyper-connectivity between brain regions, as have been observed in schizophrenia patients. [45–47] These aberrant functional connectivity patterns could have a particularly profound and lasting impact on the brain's functional organization and may contribute to psychotic symptom development.

While the global modular organization of the brain was the main focus of our study, we note that the brain regions showing region-wise changes in modular assignment were regions that are commonly associated with schizophrenia. Examining two distinct brain atlases, overlapping regions in terms of (marginal) group-effects included STG and temporal plane, anterior cingulate cortex, fusiform gyrus, and amygdala. These regions are among the most consistently implicated brain regions in early-course schizophrenia. [48–52] Examining modular network organization across levels of network resolution also indicated a change in modular assignment of STG from the

sensorimotor to the limbic module. Intriguingly, a separation of STG from the larger somatosensory community was recently reported in a study of modular brain organization in schizophrenia. [33] Other consistent abnormalities across resolutions included changes in the modular assignment of orbitofrontal cortex, striatum, and insula, in line with recent findings of salience module abnormalities in at-risk individuals. [9] Moreover, the latter study reported visual areas to extend into the limbic module. [9] Both our current and previous investigations in at-risk youth thus find primary sensory regions to become embedded in the limbic system in prodromal psychosis. These findings may fit in with theoretical models attributing psychotic symptoms to aberrant memory activations or the attribution of erroneous salience to the internal representation of a percept or memory. [53] Moreover, findings in schizophrenia patients indicate that the most prominent break-up of functional modules involves sensory, auditory, and visual areas. [33] Together, these previous and our current findings suggest that an initial separation of primary auditory and visual regions followed by a more generalized fragmentation of sensory processing may underlie disease progression in prodromal psychosis.

A number of issues should, however, be taken into account when interpreting our findings. First, physiological and head motion artifacts are known to influence fMRI-derived measures of functional connectivity. [54,55] To deal with these issues, we used the anatomical CompCor (aCompCor) method [56] for physiological noise reduction and the Artifact Detection Tool (*art*) for efficient rejection of motion and artefactual time points. [26] Second, a much-debated issue in the context of functional connectivity is the biological validity of negative, or anti-correlations. [57] A recent study indicates that when physiological and other noise sources are effectively removed, anti-correlations are present in the absence of global signal regression,

suggesting a biological origin. [58] We therefore chose to include both positively and negatively weighted connectome edges. A third and related issue is the application of thresholds in functional network analyses. In graph theoretical studies, thresholds are commonly applied to obtain a more sparsely connected representation of the functional connectome. Even when the network is examined over a range of different thresholds, the impact of imposing a threshold on the resulting graph metrics is non-trivial. Moreover, thresholding typically removes negative correlations, thereby discarding neurobiologically relevant information. [13] To avoid these limitations, we used a community detection method equipped to deal with fully weighted networks including both positive and negative edge weights. [28] Lastly, the changes in functional connectome organization observed in our study may indicate abnormalities in synchronous neural activity and modular interactions. However, given the indirect and correlational nature of functional connectivity measurements derived from resting-state fMRI, we cannot rule out the possibility that non-neural factors including hemodynamic response function variability [59,60] may have influenced our results.

This study finds that the modular organization of the functional connectome is abnormal in CHR youth that go on to develop a psychotic episode, but not in CHRs that do not develop psychosis. In addition, we show that abnormal modular connectome organization precedes overt psychosis and is predictive of psychotic development. Our results provide new insights into functional mechanisms on the connectome level that may underlie the development of psychotic symptoms and are of key interest to efforts to identify biomarkers for transition to psychosis.

Acknowledgements

This study was supported by the Ministry of Science and Technology of China (2016 YFC 1306803) and US National Institute of Mental Health (R21 MH 093294, R01 MH 101052, and R01 MH 111448). This project has received funding from the European Union's Horizon 2020 research and innovation program under Marie Skłodowska-Curie grant agreement No. 749201 (to Dr. G. Collin); Dr. Keshavan was supported by an NIMH Grant (R01 MH 64023); Drs. Shenton and McCarley were supported by a VA Merit Award.

Author contributions

LJS passed away on 7 September 2017 and RWM passed away on 27 May 2017. LJS and RWM were two of the initiators and principal investigators of the Shanghai At Risk for Psychosis (SHARP) study.

Conflict of interest

The authors declare no conflict of interest.

Supplementary Information accompanies the paper on the Molecular Psychiatry website (http://www.nature.com/mp)

References

1 Liu CH, Keshavan MS, Tronick E, Seidman LJ. Perinatal risks and childhood premorbid indicators of later psychosis: Next steps for early psychosocial interventions. *Schizophr Bull* 2015; **41**: 801–816.

2 Keshavan MS, Delisi LE, Seidman LJ. Early and broadly defined psychosis risk mental states. *Schizophr Res* 2011; **126**: 1–10.

3 Fusar-poli P, Bonoldi I, Yung AR, Borgwardt S, Kempton MJ, Valmaggia L *et al.* Predicting psychosis: Meta-analysis of transition outcomes in individuals at high clinical risk. *JAMA Psychiatry* 2012; **69**: 220–229.

4 Yung AR, McGorry PD. The Prodromal Phase of First-episode Psychosis: Past and Current Conceptualizations. *Schizophr Bull* 1996; **22**: 353–370.

5 Tandon R, Nasrallah HA, Keshavan MS. Schizophrenia, 'just the facts' 4. Clinical features and conceptualization. *Schizophr Res* 2009; **110**: 1–23.

6 Insel TR. Rethinking schizophrenia. *Nature* 2010; **468**: 187–193.

7 Simon AE, Borgwardt S, Riecher-Rössler A, Velthorst E, de Haan L, Fusar-Poli P. Moving beyond transition outcomes: Meta-analysis of remission rates in individuals at high clinical risk for psychosis. *Psychiatry Res* 2013; **209**: 266–272.

8 Schlosser DA, Jacobson S, Chen Q, Sugar CA, Niendam TA, Li G *et al.* Recovery from an at-risk state: Clinical and functional outcomes of putatively prodromal youth who do not develop psychosis. *Schizophr Bull* 2012; **38**: 1225–1233.

9 Wang C, Lee J, Ho NF, Lim JKW, Poh JS, Rekhi G *et al.* Large-Scale Network Topology Reveals Heterogeneity in Individuals With at Risk Mental State for Psychosis: Findings

From the Longitudinal Youth-at-Risk Study. *Cereb Cortex* 2017; **Epub ahead**: 1–10.

10 Anticevic A, Haut K, Murray JD, Repovs G, Yang GJ, Diehl C *et al.* Association of thalamic dysconnectivity and conversion to psychosis in youth and young adults at elevated clinical risk. *JAMA Psychiatry* 2015; **72**: 882–891.

11 Gu S, Satterthwaite TD, Medaglia JD, Yang M, Gur RE, Gur RC *et al.* Emergence of system roles in normative neurodevelopment. *Proc Natl Acad Sci USA* 2015; **112**: 13681–13686.

12 Meunier D, Lambiotte R, Bullmore ET. Modular and hierarchically modular organization of brain networks. *Front Neurosci* 2010; **4**: 200.

13 Sporns O, Betzel RF. Modular Brain Networks. *Annu Rev Psychol* 2016; **67**: 613–640.

14 Fair DA, Cohen AL, Power JD, Dosenbach NUF, Church JA, Miezin FM *et al.* Functional brain networks develop from a 'local to distributed' organization. *PLoS Comput Biol* 2009; **5**: e1000381.

15 Satterthwaite TD, Wolf DH, Ruparel K, Erus G, Elliott MA, Eickhoff SB *et al.* Heterogeneous impact of motion on fundamental patterns of developmental changes in functional connectivity during youth. *Neuroimage* 2013; **83**: 45–57.

16 Collin G, Keshavan MS. Connectome development and a novel extension to the neurodevelopmental model of schizophrenia. *Dialogues Clin Neurosci* 2018; **20**: 101–110.

17 Sporns O. Contributions and challenges for network models in cognitive neuroscience. *Nat Neurosci* 2014; **17**: 652–60.

18 Zhang T, Li H, Tang Y, Niznikiewicz MA, Shenton ME, Keshavan MS *et al.* Validating the Predictive Accuracy of the NAPLS-2 Psychosis Risk Calculator in a Clinical High-

Risk Sample From the SHARP (Shanghai At Risk for Psychosis) Program. *Am J Psychiatry* 2018; **175**: 906–908.

19 Zheng L, Wang J, Zhang T, Li H, Li C, Jiang K. The Chinese version of the SIPS/SOPS: a pilot study of reliability and validity. *Chinese Ment Heal J* 2012; **26**: 571–576.

20 Miller TJ, McGlashan TH, Rosen JL, Cadenhead K, Ventura J, Mcfarlane W *et al.* Prodromal assessment with the Structured Interview for Prodromal Syndromes and the Scale of Prodromal Symptoms: Predictive validity, interrater reliability, and training to reliability. *Schizophr Bull* 2003; **29**: 703–715.

21 Wechsler D. *WASI Manual*. Psychological Corporation, Harcourt Brace, San Antonio, TX, 1999.

22 McGlashan T, Walsh B, Woods S. *The Psychosis-Risk Syndrome: Handbook for Diagnosis and Follow-up.* New York: Oxford University Press, 2010.

23 Fornito A, Zalesky A, Breakspear M. Graph analysis of the human connectome: Promise, progress, and pitfalls. *Neuroimage* 2013; **80**: 426–444.

24 Sohn WS, Yoo K, Lee YB, Seo SW, Na DL, Jeong Y. Influence of ROI selection on resting functional connectivity: An individualized approach for resting fMRI analysis. *Front Neurosci* 2015; **9**: 1–10.

25 Fischl B. FreeSurfer. *Neuroimage* 2012; **62**: 774–81.

26 Whitfield-Gabrieli S, Nieto-Castanon A. Conn: A functional connectivity toolbox for correlated and anticorrelated brain networks. *Brain* 2012; **2**: 125–141.

27 Makris N, Meyer JW, Bates JF, Yeterian EH, Kennedy DN, Caviness VS. MRI-Based Topographic Parcellation of Human Cerebral White Matter and Nuclei. *Neuroimage* 1999;

9: 18–45.

28 Blondel VD, Guillaume J-L, Lambiotte R, Lefebvre E. Fast unfolding of communities in large networks. *J Stat Mech* 2008; : P10008.

29 Rubinov M, Sporns O. Weight-conserving characterization of complex functional brain networks. *Neuroimage* 2011; **56**: 2068–2079.

30 Good BH, de Montjoye YA, Clauset A. Performance of modularity maximization in practical contexts. *Phys Rev E* 2010; **81**: 46106.

31 Doron KW, Bassett DS, Gazzaniga MS. Dynamic network structure of interhemispheric coordination. *PNAS* 2012; **109**: 18661–18668.

32 Traud AL, Kelsic ED, Mucha PJ, Porter MA. Comparing Community Structure to Characteristics in Online Collegiate Social Networks. *SIAM Rev* 2008; **53**: 526–543.

33 Bordier C, Nicolini C, Forcellini G, Bifone A. Disrupted modular organization of primary sensory brain areas in schizophrenia. *NeuroImage Clin* 2018; **18**: 682–693.

34 Lerman-Sinkoff DB, Barch DM. Network community structure alterations in adult schizophrenia: Identification and localization of alterations. *NeuroImage Clin* 2016; **10**: 96–106.

35 Hoffman R, Dobschka S. Cortical Pruning and the Development of Schizophrenia: A Computer Model. *Schizophr Bull* 1989; **15**: 477–490.

36 Hoffman R, McGlashan T. Parallel Distributed Processing and the Emergence of Schizophrenic Symptoms. *Schizophr Bull* 1993; **19**: 119–140.

37 Hoffman RE, McGlashan TH. Synaptic elimination, neurodevelopment, and the mechanism of hallucinated ‘voices’ in schizophrenia. *Am J Psychiatry* 1997; **154**: 1683–

1689.

38 David AS. Dysmodularity: a neurocognitive model for schizophrenia. *Schizophr Bull* 1994; **20**: 249–255.

39 Yu Q, Plis SM, Erhardt EB, Allen EA, Sui J, Kiehl KA *et al.* Modular Organization of Functional Network Connectivity in Healthy Controls and Patients with Schizophrenia during the Resting State. *Front Syst Neurosci* 2012; **5**: 1–16.

40 Van den Heuvel MP, Sporns O, Collin G, Scheewe T, Mandl RCW, Cahn W *et al.* Abnormal rich club organization and functional brain dynamics in schizophrenia. *JAMA psychiatry* 2013; **70**: 783–92.

41 Schmidt A, Crossley NA, Harrisberger F, Smieskova R, Lenz C, Riecher-Rössler A *et al.* Structural network disorganization in subjects at clinical high risk for psychosis. *Schizophr Bull* 2017; **43**: 583–591.

42 Alexander-Bloch AF, Gogtay N, Meunier D, Birn R, Clasen L, Lalonde F *et al.* Disrupted modularity and local connectivity of brain functional networks in childhood-onset schizophrenia. *Front Syst Neurosci* 2010; **4**: 147.

43 Supekar K, Musen M, Menon V. Development of large-scale functional brain networks in children. *PLoS Biol* 2009; **7**: e1000157.

44 Casey B, Jones R, Somerville L. Braking and Accelerating of the Adolescent Brain. *J Res Adolesc* 2011; **21**: 21–33.

45 Skudlarski P, Jagannathan K, Anderson K, Stevens MC, Calhoun VD, Skudlarska BA *et al.* Brain connectivity is not only lower but different in schizophrenia: a combined anatomical and functional approach. *Biol Psychiatry* 2010; **68**: 61–9.

46 Pettersson-Yeo W, Allen P, Benetti S, McGuire P, Mechelli A. Dysconnectivity in schizophrenia: where are we now? *Neurosci Biobehav Rev* 2011; **35**: 1110–24.

47 Zalesky A, Cocchi L, Fornito A, Murray MM, Bullmore E. Connectivity differences in brain networks. *Neuroimage* 2012; **60**: 1055–1062.

48 Honea R, Sc B, Crow TJ, Ph D, Passingham D, Ph D *et al.* Regional Deficits in Brain Volume in Schizophrenia : A Meta-Analysis of Voxel-Based Morphometry Studies. *Am J Psychiatry* 2005; **162**: 2233–2245.

49 Glahn DC, Laird AR, Ellison-Wright I, Thelen SM, Robinson JL, Lancaster JL *et al.* Meta-Analysis of Gray Matter Anomalies in Schizophrenia: Application of Anatomic Likelihood Estimation and Network Analysis. *Biol Psychiatry* 2008; **64**: 774–781.

50 Vita A, De Peri L, Deste G, Sacchetti E. Progressive loss of cortical gray matter in schizophrenia: A meta-analysis and meta-regression of longitudinal MRI studies. *Transl Psychiatry* 2012; **2**: e190-13.

51 Shenton ME, Dickey CC, Frumin M, Mccarley RW. A review of MRI findings in schizophrenia. *Schizophr Res* 2001; **49**: 1–52.

52 Jung WH, Borgwardt S, Fusar-Poli P, Kwon JS. Gray matter volumetric abnormalities associated with the onset of psychosis. *Front Psychiatry* 2012; **3**: 1–21.

53 Tracy DK, Shergill SS. Mechanisms underlying auditory hallucinations - understanding perception without stimulus. *Brain Sci* 2013; **3**: 642–669.

54 Satterthwaite TD, Wolf DH, Loughead J, Ruparel K, Elliott MA, Hakonarson H *et al.* Impact of in-scanner head motion on multiple measures of functional connectivity: Relevance for studies of neurodevelopment in youth. *Neuroimage* 2012; **60**: 623–632.

55 Power JD, Barnes KA, Snyder AZ, Schlaggar BL, Petersen SE. Spurious but systematic correlations in functional connectivity MRI networks arise from subject motion. *Neuroimage* 2012; **59**: 2142–2154.

56 Behzadi Y, Restom K, Liau J, Liu TT. A component based noise correction method (CompCor) for BOLD and perfusion based fMRI. *Neuroimage* 2007; **37**: 90–101.

57 Murphy K, Birn RM, Handwerker DA, Jones TB, Bandettini PA. The impact of global signal regression on resting state correlations: are anti-correlated networks introduced? *Neuroimage* 2009; **44**: 893–905.

58 Chai XJ, Castañán AN, Öngür D, Whitfield-Gabrieli S. Anticorrelations in resting state networks without global signal regression. *Neuroimage* 2012; **59**: 1420–1428.

59 Murphy K, Birn RM, Bandettini PA. Resting-state FMRI confounds and cleanup. *Neuroimage* 2013; **80**: 349–359.

60 Rangaprakash D, Wu GR, Marinazzo D, Hu X, Deshpande G. Hemodynamic response function (HRF) variability confounds resting-state fMRI functional connectivity. *Magn Reson Med* 2018; **80**: 1697–1713.

Table 1. Demographic and clinical characteristics

Statistical comparison was performed using analysis of variance (ANOVA) tests for continuous, and chi-squared tests for categorical variables.

	CHR+ *N* = 23	CHR- *N* = 135	Controls *N* = 93	Statistics
Age, mean (sd) [range]	19.2 (5.2) [14 – 34]	18.7 (4.9) [13 – 32]	18.7 (4.6) [12 – 35]	$F = 0.10$, $p = 0.905$
Sex, male/female	16 / 7	64 / 71	49 / 44	$\chi^2 = 3.96$, $p = 0.138$
Education in years, mean (sd) [range]	10.3 (2.2) [7 – 16]	10.5 (2.9) [4 – 19]	10.8 (2.3) [6 – 17]	$F = 0.52$, $p = 0.597$
IQ, mean (sd) [range]	92.1 (19.0) [52 – 112]	99.9 (11.2) [67 – 128]	104.2 (11.1) [75 – 133]	$F = 8.53$, $p < 0.001$[1]
Baseline SIPS scores				
Positive, mean (sd) [range]	10.0 (3.3) [4 – 17]	10.1 (3.7) [0 – 21]		$F = 0.03$, $p = 0.871$
Negative, mean (sd) [range]	12.1 (6.4) [3 – 26]	11.6 (6.1) [1 – 27]		$F = 0.16$, $p = 0.687$
Disorganized, mean (sd) [range]	6.5 (3.0) [2 – 13]	6.6 (3.3) [1 – 19]		$F = 0.02$, $p = 0.891$
General, mean (sd) [range]	9.0 (2.9) [3 – 14]	9.1 (3.3) [1 – 17]		$F = 0.01$, $p = 0.902$
Total, mean (sd) [range]	37.6 (10.7) [16 – 65]	37.3 (10.9) [13 – 79]		$F = 0.01$, $p = 0.922$
Psychotropic medication				
At inclusion, N (%)	1 (4.3)	6 (4.4)		$\chi^2 < 0.01$, $p = 0.983$
At baseline MRI, N (%)	7 (30.4)	22 (16.3)		$\chi^2 = 2.62$, $p = 0.105$
Antipsychotics, N (%)	6 (26.1)	18 (13.3)		$\chi^2 = 2.48$, $p = 0.115$
Antidepressants, N (%)	2 (8.7)	5 (3.7)		$\chi^2 = 1.57$, $p = 0.282$
Other, N (%)	1 (4.3)	1 (0.7)		$\chi^2 = 2.05$, $p = 0.153$
GAF highest, mean (sd) [range]	77.6 (2.6) [73 – 83]	77.3 (4.9) [47 – 85]		$F = 0.08$, $p = 0.776$
GAF current, mean (sd) [range]	52.7 (7.7) [43 – 78]	54.1 (8.4) [21 – 76]		$F = 0.58$, $p = 0.449$

[1] post-hoc analysis (Tukey-Kramer) indicates a significant IQ difference between each pair of subject groups (HC vs. CHR+, $p = 0.002$; HC vs. CHR-, $p = 0.022$; CHR- vs CHR+, $p = 0.039$).

Figures

Figure 1 Image preprocessing and connectome analysis steps

Overview of image preprocessing (A), connectome reconstruction (B), and modular community detection analysis (C). Of note, the colors of the modules shown in the connectivity matrices in panel C correspond to the modules as shown in Figure 2A.

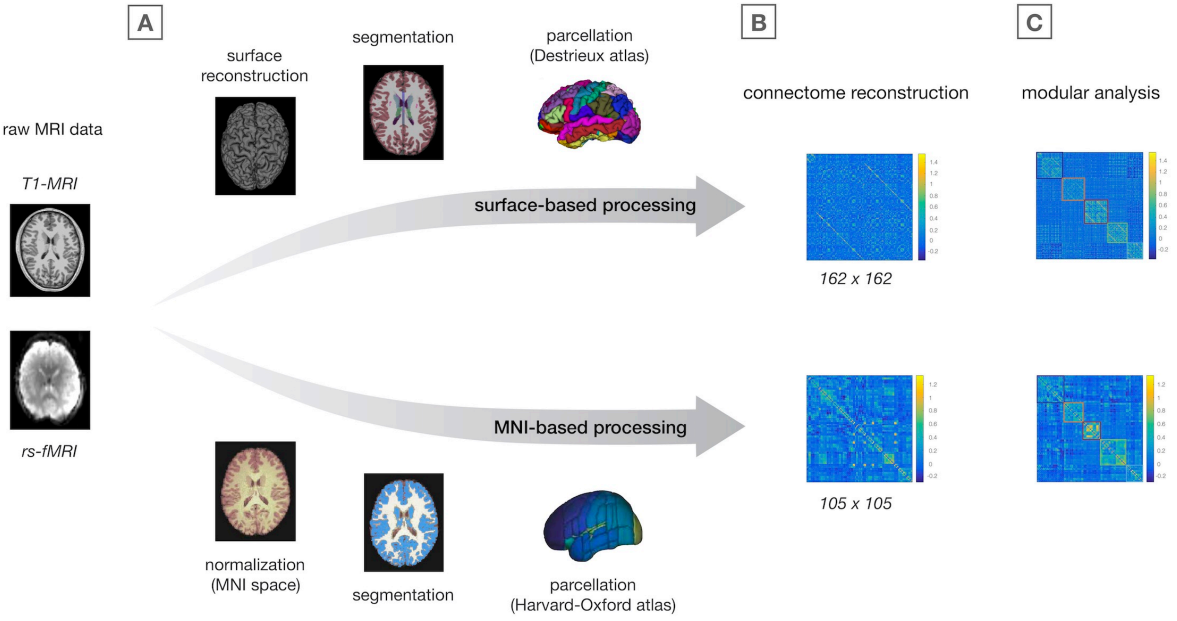

Figure 2 Modular organization of the functional connectome

A) Modular partitions of group-networks, plotted on cortical surface from superior, lateral, medial, and inferior angle, and subcortical structures (top to bottom row respectively). Colors indicate separate modules, with the prefrontal central-executive (CE) module in dark blue, the central sensorimotor (SM) module in green, the posterior visual (VIS) module in red, the (para)limbic (LIM) module in orange, the medial default mode (DM) module in light blue, and the cingulo-opercular (CO) module in yellow. B) Degree of similarity to average healthy network (S_R) for individual subjects. Jittered data are plotted for each group, with mean (sd) values represented by the box behind the raw data. * indicates significant group-difference.

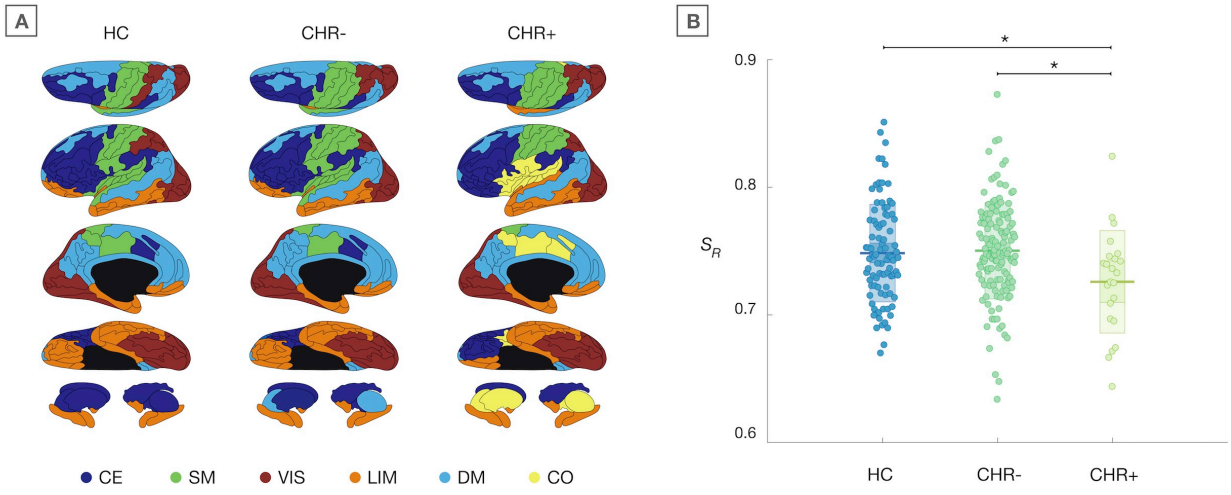

Figure 3 Regional findings of abnormal module assignment

Surface plots showing exploratory regional findings (S_{Rnode}) at uncorrected $p < .05$ for surface-based (left) and MNI-based (right) methods respectively. * FDR-corrected significant effect for right superior temporal gyrus, anterior division.

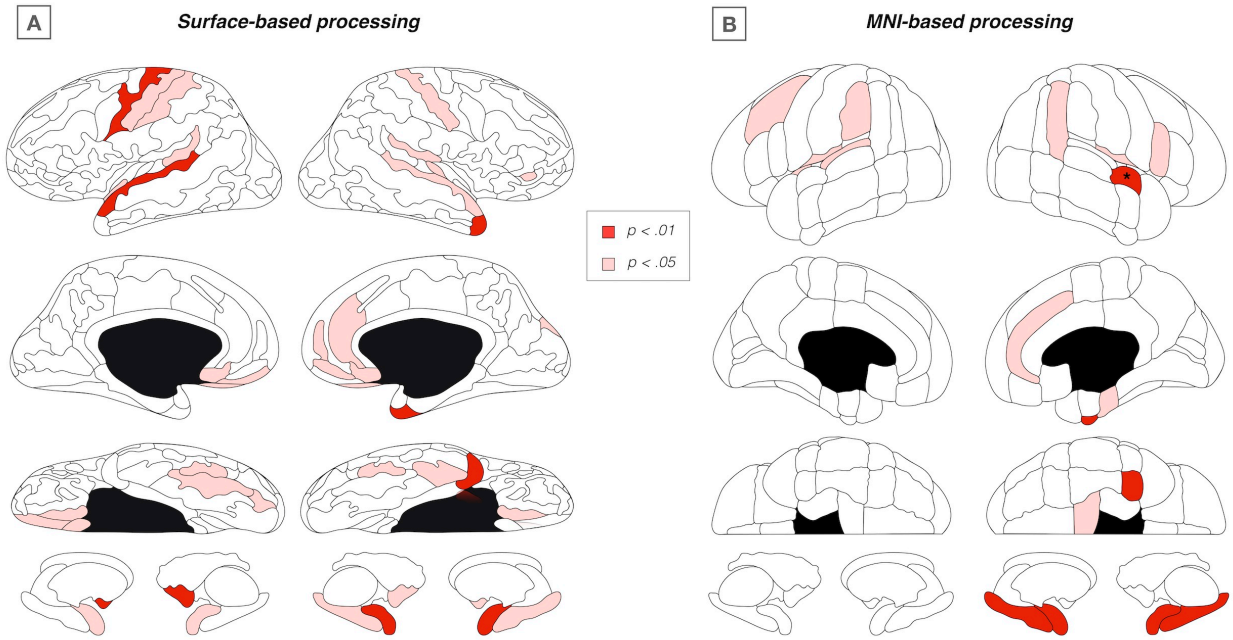

Figure 4 Psychosis-free survival for typical vs. atypical baseline connectome organization

Kaplan-Meier plot showing psychosis-free survival functions for CHRs with above-average (red) and below-average (blue) levels of S_R (reflecting typical and atypical connectome organization respectively) as a functional of time since baseline (days).

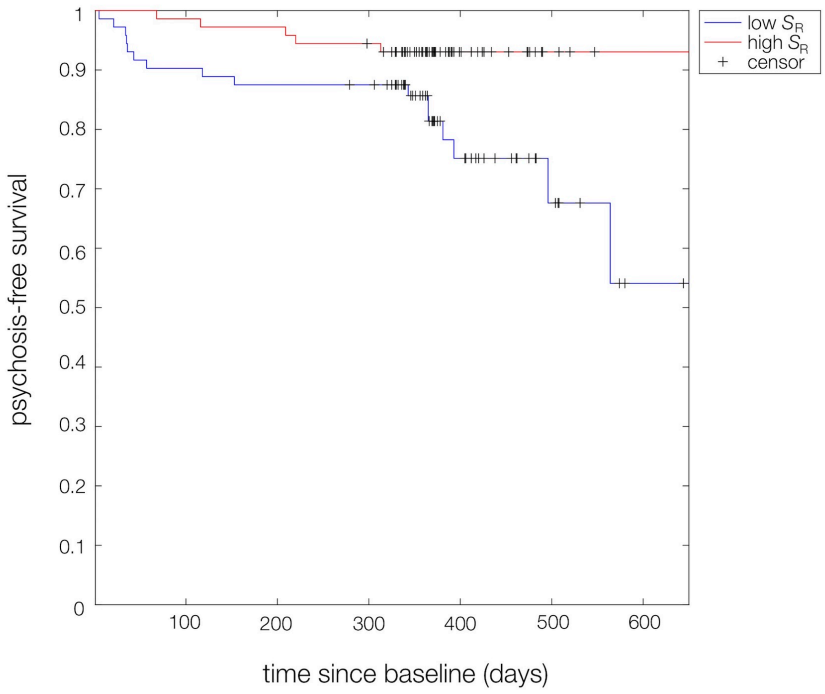

SUPPLEMENTARY INFORMATION

Functional Connectome Organization Predicts Conversion to Psychosis in Clinical High-Risk Youth from the SHARP Program

Guusje Collin, MD, PhD [1,2,3]; Larry J. Seidman, PhD [1,†]; Matcheri S. Keshavan, MD [1]; William S. Stone, PhD [1]; Zhenghan Qi, MD, PhD [1,4]; Tianhong Zhang, MD, PhD [5]; Yingying Tang, PhD [5]; Huijun Li, PhD [6]; Sheeba Arnold Anteraper, PhD [2,7]; Margaret A. Niznikiewicz, PhD [8]; Robert W. McCarley, MD [8,†]; Martha E. Shenton, PhD [3,9,10]; Jijun Wang, MD [5]; Susan Whitfield-Gabrieli, PhD [2,11]

[1] Department of Psychiatry, Beth Israel Deaconess Medical Center, Harvard Medical School, Boston, MA, USA; [2] McGovern Institute for Brain Research, Department of Brain and Cognitive Sciences, Massachusetts Institute of Technology, Cambridge, MA, USA; [3] Psychiatry Neuroimaging Laboratory, Department of Psychiatry, Brigham and Women's Hospital, Harvard Medical School, Boston, MA, USA; [4] Department of Linguistics and Cognitive Science, University of Delaware, Newark, DE, USA; [5] Shanghai Key Laboratory of Psychotic Disorders, Shanghai Mental Health Center, Shanghai Jiao Tong University School of Medicine, Shanghai, China; [6] Florida A&M University, Department of Psychology, Tallahassee, FL, USA; [7] Alan and Lorraine Bressler Clinical and Research Program for Autism Spectrum Disorder, Massachusetts General Hospital, Boston MA, USA; [8] Department of Psychiatry, VA Boston Healthcare System, Brockton Division, Brockton, MA, USA; [9] Research and Development, VA Boston Healthcare System, Brockton Division, Brockton, MA, USA; [10] Department of Radiology, Brigham and Women's Hospital, Harvard Medical School, Boston, MA, USA; [11] Poitras Center for Affective Disorders, Department of Brain and Cognitive Sciences, Massachusetts Institute of Technology, Cambridge, MA, USA

Supplementary Information 1.1 Sample selection

Study and recruitment details

The Shanghai at risk for psychosis (SHARP) program recruited participants between August 2012 and January 2017. The first phase of the SHARP program recruited 100 CHR youths between August 2012 and May 2014 (R21 MH 093294-01). The second phase recruited 200 CHRs between June 2014 and January 2017 (R01 MH 101052-01). [1] Out of the total 300 CHRs and 138 matched healthy controls (HCs), imaging data was available for 260 subjects. Nine of these subjects were excluded due to low-quality neuroimaging data, resulting in a total of 251 subjects included in the current study. CHRs were selected among help-seeking individuals at the SMHC using well validated procedures [2] and HCs were recruited from the local community. Inclusion was restricted to individuals aged 15 to 45 years who were able to understand the study. Informed consent was obtained after oral and written explanation of all study procedures. For participants below age 18, informed consent was obtained from the parents and assent from the (minor) participant. No participants had a history of substance abuse or dependence.

Power analysis. A post-hoc power analysis conducted using G*Power v3.1 (http://www.gpower.hhu.de) showed that the current sample of 251 subjects achieved 80% power to detect Cohen's *f* effect sizes as small as $f = 0.2$ at the standard alpha level of $p < .05$ (two-tailed), meaning that the sample has enough power to detect a small to medium effect.

Supplementary Information 1.2 Image preprocessing

Surface-based method

Freesurfer (v6.0) software (https://surfer.nmr.mgh.harvard.edu) was used to process T1-weighted MRI scans, including segmentation of grey and white matter tissue and parcellation of the cortex and subcortical grey matter into a total of 162 bilateral brain regions. These regions included 148 cortical regions comprising the Destrieux atlas [3] and 14 subcortical structures including bilateral thalamus, hippocampus, amygdala, nucleus accumbens, caudate nucleus, putamen and global pallidus. The CONN Toolbox (17d) [4] (https://www.nitrc.org/projects/conn) was used for realignment, coregistration, and slice timing correction of rs-fMRI scans. To address spurious correlations in BOLD timeseries due to head motion, the Artifact Detection Tool (ART, http://www.nitrc.org/projects/artifact_detect) was used to identify problematic time points. Outliers (i.e., artefactual timepoints) were defined as volumes showing head displacement in the x, y, or z direction greater than 1 mm relative to the previous frame or global mean intensity in the image greater than 3 standard deviations from the mean intensity for the entire resting-state scan. Timeseries were corrected through linear regression for motion (captured by 3 rotational, 3 translational, and 1 composite motion parameter), artefactual covariates, and signals within white matter (3 PCA parameters) and CSF (3 PCA parameters) masks. The resulting timeseries were band-pass filtered (0.008 Hz – 0.09 Hz).

MNI-based method

For the additional processing method, CONN software (17d) was used to preprocess T1-weighted and rs-fMRI scans. Preprocessing of T1-weighted scans included segmentation of grey and white

matter tissue, normalization to Montreal Neurological Institute (MNI) space, and using the Harvard-Oxford atlas to divide the cerebrum into a total of 105 brain regions, including 91 cortical brain regions and the same 14 subcortical structures. Rs-fRMI scans were realigned, slice-timing corrected, normalized to MNI space, and smoothed (6mm FWHM Gaussian filter). Potential spurious correlations were again assessed using ART, defining outliers as specified in the previous paragraph. Time-series were again corrected through linear regression for motion, artefactual covariates, and signals within white matter (3 PCA parameters) and CSF (3 PCA parameters) masks, with resulting timeseries being band-pass filtered (0.008 Hz – 0.09 Hz).

Motion parameters and artefactual timepoints

Analysis of variance (ANOVA) was used to test group-differences in subject motion and the number of artifactual timepoints identified by ART for statistical significance. For the surface-based data, there were no significant group-differences in the composite motion parameter ($F_{(2, 250)} = 1.15$, $p = .318$) or the number of artefactual timepoints ($F_{(2, 250)} = 0.18$, $p = .832$). For the MNI-based data, there were also no significant group-differences in motion ($F_{(2, 250)} = 0.22$, $p = .802$) or the number of artefactual timepoints ($F_{(2, 250)} = 0.05$, $p = .954$).

Supplementary Information 1.3 Modular connectome analysis

Rand similarity coefficient

The Rand similarity coefficient (Network Community Toolbox; http://commdetect.weebly.com) reflects the fraction of node pairs that are identified in the same way across two partitions: i.e., either both belonging to the same community in two partitions or both belonging to different communities in two partitions. Bound between 0 (no equal pair placements) and 1 (identical partitions), S_R is an intuitive measure of the overall similarity of two network partitions.

Region-specific alterations in modular organization

To assess which brain regions are most abnormal in terms of module assignment, individual networks were compared to an average healthy network, determining for each node the fraction of neighboring nodes with equal module assignment. This measure, S_{Rnode}, reflects how many of a region's neighbors are assigned in the same way in the individual network relative to the healthy network (i.e., with the region and its neighbor either belonging to the same module in both networks or belonging to separate modules in both networks).

Validation analysis excluding individual HCs

To ensure that HC results were not biased by the fact that these subjects contributed to the average HC network, we ran an additional analysis in which we constructed 93 separate HC networks, each time leaving out one HC and comparing that subject's modular network partition to the HC network based on the 92 other HCs. Comparing these values against CHRs confirmed the significantly lower value of S_R in CHR+ relative to HC ($F_{(1, 110)} = 4.43$, $p = .038$).

Modular analysis using MNI-based data

Repeating individual network analyses using MNI-based data largely corroborated our main findings. The Rand similarity coefficient (S_R), reflecting the level of similarity between modular partitions of individual subjects and the HC network, again showed a significant main effect of group $F_{(2, 245)} = 6.75$, $p = .001$), with modular network organization being less similar to an average HC network in CHR+ than in CHR- ($F_{(1, 152)} = 9.04$, $p = .003$) (Supplementary Figure 3). However, contrary to our primary findings, the post-hoc difference between CHR+ and HCs was not statistically significant for the MNI-based data. Possibly, the surface-based method is more sensitive to pick up group-differences, because it involves a more fine-grained parcellation of the cortex or because it does not include spatial normalization to standard space which may remove some of the inter-subject anatomical variability.

Modular analysis across resolutions

We reassessed our results across different levels of resolution parameter γ. To this end, we varied γ and performed the main group-analysis (i.e., assessing similarity of individual modular partitions to an average healthy network using Rand similarity coefficients and comparing S_R between subject groups) for each level of γ. This analysis shows that our main results hold for a range of gamma ($\gamma = 1.2 – 1.6$) (Supplementary Figure 1). Across resolutions, the most consistent group-differences are modular abnormalities of the CHR+ network involving mainly orbito-frontal, superior temporal, sensorimotor, insular, and striatal regions (Supplementary Figure 2).

Consensus partitioning

Several methods exist to identify optimal modular partitions among an iterative set of modular partitions. As an alternative to approach described in the main text (i.e., selecting the partition associated with the highest level of Q), we also explored a consensus similarity method that identifies a single representative modular partition that is most similar to all other partitions in the iterative set. [6] To derive consensus modular partitions, we again computed an iterative set of modular partitions for the group-averaged networks and then used the consensus similarity algorithm from the Network Community Toolbox (http://commdetect.weebly.com) to identify a single representative partition that is most similar to all other partitions in the iterative set. We used the same procedure to derive consensus partitions for individual participants.

To assess how similar the consensus partitions were to the original partitions (as reported in the main text), we calculated Rand similarity coefficients (S_R) between the original partitions and the newly created consensus partitions. This analysis showed that the consensus partitions for group-averaged networks were highly similar to our original partitions, as indicated by S_R of 0.99, 0.96, and 0.98 for converters, nonconverters, and controls respectively. Individual partitions derived using both methods were also highly similar, as shown by a mean (sd) S_R of 0.94 (0.05), and with no significant differences in S_R between subject groups ($F = 0.97$, $p = .38$).

Next, we performed a reanalysis of our main findings using network partitions derived from the consensus partitioning approach. Specifically, we compared individual consensus partitions to the consensus partition of the group-averaged HC network using S_R to determine how similar each individual subject's consensus partition was to that of an average healthy network. Statistical analysis of similarity coefficients indicated a trend-level effect of group

($F_{(2,245)} = 2.56$, $p = .079$), with post-hoc bivariate comparisons indicating consensus partitions of CHR+ to be less similar to an average healthy network than those of HCs ($F_{(1,110)} = 4.22$, $p = .042$) and CHR- ($F_{(1,152)} = 4.98$, $p = .027$).

Supplementary Information 1.4 Statistical analysis

Analysis of Covariance - assumptions

Assumptions for the use of Analysis of Covariance (ANCOVA) for group-comparisons were met: Shapiro Wilk tests indicated that S_R values were normally distributed within each group (all $p > .05$); Levene's test for equality of variance indicated equal variance between groups ($F = 0.145$, $p = .86$).

Supplementary Information 1.5 Psychosis-free survival analysis

Survival analysis using MNI-based data

Using *MNI-based* data also revealed significantly worse psychosis-free survival for CHRs with atypical modular connectome organization at baseline (z = 2.67, p = .008; Hazard ratio = 3.6, log rank tests) (Supplementary Figure 4). Cox regression analysis again showed baseline modular connectome organization (z = -2.06, p = .040), IQ (z = -2.05, p = .041) and sex (z = 2.56, p = .011) to predict time to conversion.

References

1 Zhang T, Li H, Tang Y, Niznikiewicz MA, Shenton ME, Keshavan MS *et al.* Validating the Predictive Accuracy of the NAPLS-2 Psychosis Risk Calculator in a Clinical High-Risk Sample From the SHARP (Shanghai At Risk for Psychosis) Program. *Am J Psychiatry* 2018; **175**: 906–908.

2 McGlashan T, Walsh B, Woods S. *The Psychosis-Risk Syndrome: Handbook for Diagnosis and Follow-up.* New York: Oxford University Press, 2010.

3 Destrieux C, Fischl B, Dale A, Halgren E. Automatic parcellation of human cortical gyri and sulci using standard anatomical nomenclature. *Neuroimage* 2010; **53**: 1–15.

4 Whitfield-Gabrieli S, Nieto-Castanon A. Conn: A functional connectivity toolbox for correlated and anticorrelated brain networks. *Brain* 2012; **2**: 125–141.

5 Blondel VD, Guillaume J-L, Lambiotte R, Lefebvre E. Fast unfolding of communities in large networks. *J Stat Mech* 2008; : P10008.

6 Doron KW, Bassett DS, Gazzaniga MS. Dynamic network structure of interhemispheric coordination. *PNAS* 2012; **109**: 18661–18668.

SUPPLEMENTARY FIGURES

Functional Connectome Organization Predicts Conversion to Psychosis in Clinical High-Risk Youth from the SHARP Program

Guusje Collin, MD, PhD [1,2,3]; Larry J. Seidman, PhD [1,†]; Matcheri S. Keshavan, MD [1]; William S. Stone, PhD [1]; Zhenghan Qi, MD, PhD [1,4]; Tianhong Zhang, MD, PhD [5]; Yingying Tang, PhD [5]; Huijun Li, PhD [6]; Sheeba Arnold Anteraper, PhD [2,7]; Margaret A. Niznikiewicz, PhD [8]; Robert W. McCarley, MD [8,†]; Martha E. Shenton, PhD [3,9,10]; Jijun Wang, MD [5]; Susan Whitfield-Gabrieli, PhD [2,11]

[1] Department of Psychiatry, Beth Israel Deaconess Medical Center, Harvard Medical School, Boston, MA, USA; [2] McGovern Institute for Brain Research, Department of Brain and Cognitive Sciences, Massachusetts Institute of Technology, Cambridge, MA, USA; [3] Psychiatry Neuroimaging Laboratory, Department of Psychiatry, Brigham and Women's Hospital, Harvard Medical School, Boston, MA, USA; [4] Department of Linguistics and Cognitive Science, University of Delaware, Newark, DE, USA; [5] Shanghai Key Laboratory of Psychotic Disorders, Shanghai Mental Health Center, Shanghai Jiao Tong University School of Medicine, Shanghai, China; [6] Florida A&M University, Department of Psychology, Tallahassee, FL, USA; [7] Alan and Lorraine Bressler Clinical and Research Program for Autism Spectrum Disorder, Massachusetts General Hospital, Boston MA, USA; [8] Department of Psychiatry, VA Boston Healthcare System, Brockton Division, Brockton, MA, USA; [9] Research and Development, VA Boston Healthcare System, Brockton Division, Brockton, MA, USA; [10] Department of Radiology, Brigham and Women's Hospital, Harvard Medical School, Boston, MA, USA; [11] Poitras Center for Affective Disorders, Department of Brain and Cognitive Sciences, Massachusetts Institute of Technology, Cambridge, MA, USA

Supplementary Figure 1. Group-effects across a range of γ.

Plot showing mean (sd) Rand similarity coefficients per group as a function of network resolution (γ), illustrating that significant group-effects are present across a range of γ (with * indicating significant effects).

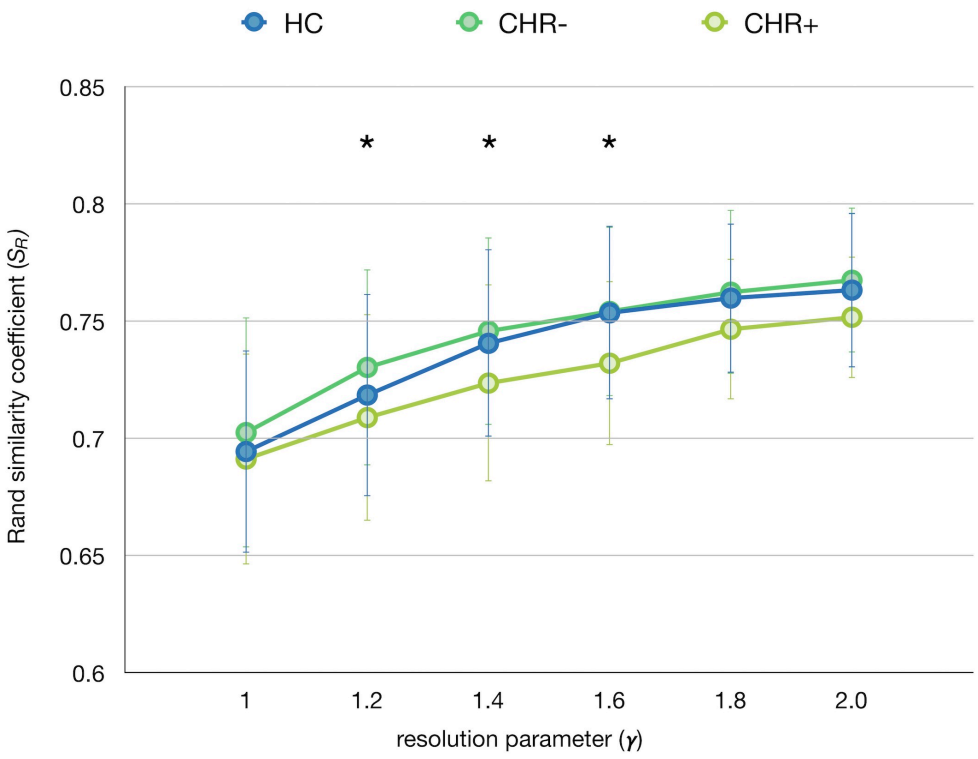

Supplementary Figure 2. Modular partitions per group across a range of γ.

Modular partitions of group-networks, plotted on a cortical and subcortical rendering, for three levels of network resolution (i.e., $\gamma = 1.2$, 1.4, and 1.6) for which significant group-effects were found (see Supplementary Figure 1). CE = Central Executive; SM = Sensorimotor; VIS = Visual; LIM = Limbic; DM = Default Mode; CO = Cingulo-opercular.

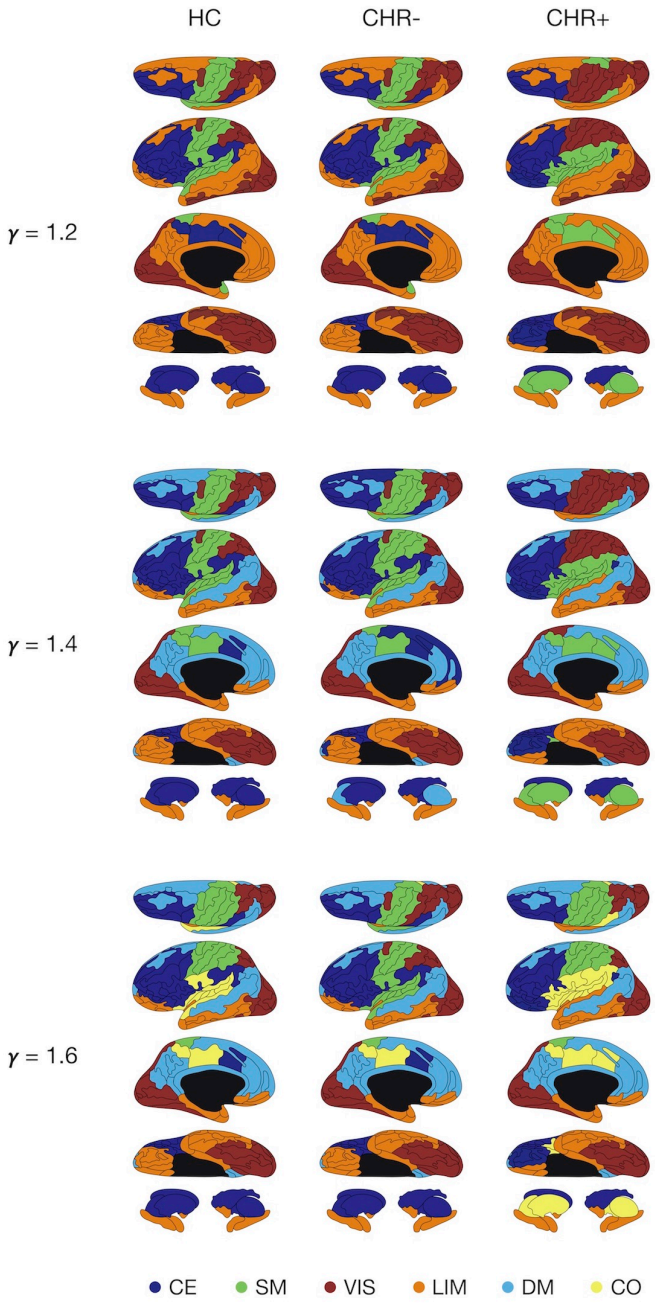

Supplementary Figure 3. Similarity in modular organization to healthy network (MNI-based). Plot of S_R levels (reflecting the degree of similarity to HC network) per subject group for MNI-processed data. Jittered data are plotted for each group, with mean (sd) values represented by box behind raw data. * indicates significant group-difference.

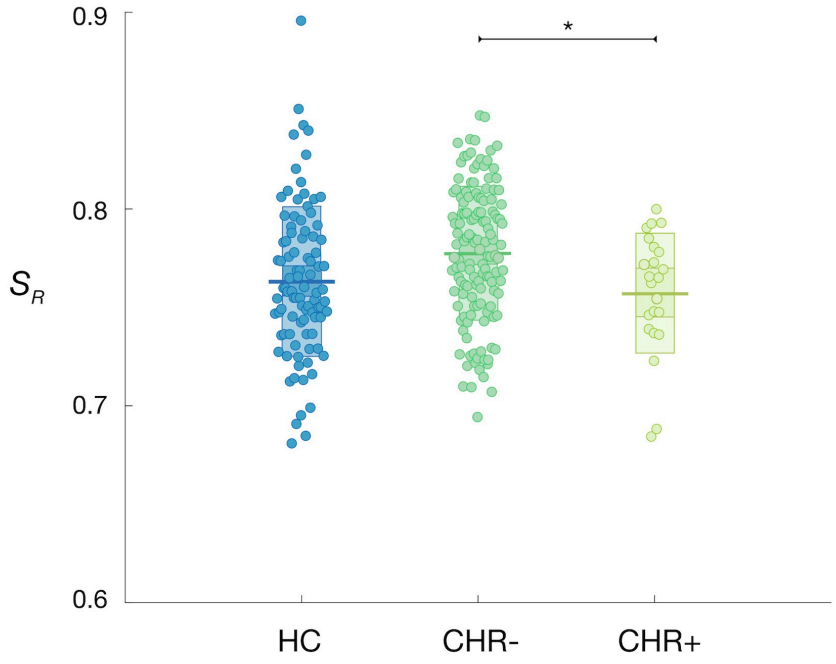

Supplementary Figure 4. Psychosis-free survival for typical vs. atypical connectome organization (MNI-based).

Kaplan-Meier plot showing psychosis-free survival functions for CHRs with above-average (red) and below-average (blue) levels of S_R (reflecting typical and atypical connectome organization respectively) as a functional of time since baseline (days), for MNI-processed data.